Deep Learning-based Channel Predictor for RIS-assisted NOMA

Eduardo F. S. L. Henriques, Rafael S. Chaves, and Paulo S. R. Diniz

***Abstract*— This paper explores the integration of non-orthogonal multiple access (NOMA) and reconfigurable intelligent surfaces (RIS) as key technologies to address the wireless communications challenges. NOMA improves spectral efficiency by enabling resource sharing among multiple users, while RIS enhances signal quality and coverage with lower energy consumption. However, this integration introduces complexity and non-linearity in channel estimation. To tackle this, we employ deep learning (DL) models, specifically convolutional neural networks (CNN) and long short term memory (LSTM) networks, to improve channel state prediction. Our main contribution is a new DL model with additional layers for more accurate magnitude and phase prediction. Simulations demonstrate that the proposed model reduces average inference time by 17%, decreases the number of training parameters by over 35%, and showcases signal-to-noise ratio (SNR) gains for fixed bit-error rate (BER).**

***Keywords*— NOMA, RIS, Channel Estimation, CNN, LSTM**

I. Introduction

As we approach the transition from fifth generation (5G) to the forthcoming sixth generation (6G) networks, the telecommunications industry is experiencing an unprecedented demand for higher data rates, lower latency, and enhanced reliability [1], [2]. These demands require innovative solutions to meet the increasing data consumption [3]. Central to these advancements are non-orthogonal multiple access (NOMA) and reconfigurable intelligent surfaces (RIS) [4]–[6]. NOMA, which differs from traditional orthogonal multiple access (OMA) techniques [7], [8] by enabling multiple users to share the same communication resources, allowing higher spectral efficiency (SE). On the other hand, RIS has the potential to intelligently manipulate the signal propagation to optimally achieve quality and coverage with reduced energy usage [9]–[12]. Thus, there is no competition between NOMA and RIS. Rather, they can be integrated, providing a significant advantage to NOMA by increasing its throughput performance through improved signal quality and coverage [4], [13].

The integration of RIS in NOMA communication systems enhances communication capacity but introduces significant channel estimation complexity due to the increased number of channel coefficients and the non-linear interactions between multiple users and RIS elements [14]. Traditional methods may struggle to handle this complexity [15], making them less effective and computationally expensive. To overcome these challenges, this work employs advanced deep learning (DL) techniques [16], using convolutional neural networks (CNN) [17] for robust feature extraction and long short term memory (LSTM) [18] networks for effective sequential data processing. This AI-driven approach aims to improve channel estimation by capturing both the magnitude and phase of received signals, thereby enhancing adaptability, data handling capacity, and reliability in RIS-NOMA systems.

Key contributions of this paper include exploring the synergy of RIS-NOMA, incorporating phase prediction within the DL architecture for improved channel estimation accuracy, introducing reduced-complexity DL architecture with modified pooling layers to optimize performance, and conducting a detailed bit-error rate (BER) evaluation with successive interference cancellation (SIC) technique to validate the model's effectiveness in practical applications.

The remainder of the paper is organized as follows: Section II describes the downlink transmission for a RIS-assisted NOMA system. Section III details the proposed DL architecture for channel estimation. In Section IV, simulation results evaluate the BER over varying signal-to-noise ratio (SNR) values comparing the proposed channel predictor with the state-of-the-art. Finally, the conclusion is drawn in Section V.

Notations: Vectors and matrices are represented by boldface lowercase and uppercase letters, respectively. The notation $\mathbf{X}^{\mathrm{T}}$ and $\mathbf{X}^{\mathrm{H}}$ stand for transpose, and Hermitian operations on $\mathbf{X}$, respectively. The symbols $\mathbb{C}$, $\mathbb{R}$, $\mathbb{R}_+$, and $\mathbb{N}$ denote the sets of complex, real, non-negative real, and natural numbers, respectively. The set $\mathbb{C}^{M\times K\times L}$ denotes all $M\times K\times L$ matrices comprised of complex-valued entries. The symbol $\mathcal{CN}(\mathbf{m},\mathbf{C})$ denotes a circularly symmetric Gaussian distribution with mean $\mathbf{m}$ and covariance matrix $\mathbf{C}$. The symbol $\mathbb{E}[X]$ denotes a the expected value of a random variable X.

II. System Model

Consider a NOMA system operating in downlink transmission with a single-antenna base station (BS) aided by a RIS equipped with L passive reflecting elements and serving M single-antenna user equipments (UEs) as illustrated in Fig. 1. The BS transmits the superposed signal $x(n)$, given by

$$x(n)=\sum_{m=1}^{M}\sqrt{p_m}x_m(n), \tag{1}$$

where $n\in\{1,2,\ldots,N\}$ is the time in samples with $N\in\mathbb{N}$ being the transmission duration, $x_m(n)\in\mathcal{C}\subset\mathbb{C}$ is the transmitted signal from a generic constellation, and $p_m\in\mathbb{R}_+$

Eduardo F. S. L. Henriques, Department of Electronics and Computer Engineering (DEL), Universidade Federal do Rio de Janeiro (UFRJ), Rio de Janeiro, RJ, Brazil, eduardo.henriques@poli.ufrj.br; Rafael S. Chaves, Coordenação do Curso de Engenharia de Telecomunicações (CCGTEL), Centro Federal de Educação Tecnológica Celso Suckow da Fonseca (CEFET-RJ), Rio de Janeiro, RJ, Brazil, e-mail: rafael.chaves@cefet-rj.br; Paulo S. R. Diniz, Department of Electronics and Computer Engineering (DEL), Universidade Federal do Rio de Janeiro (UFRJ), Rio de Janeiro, RJ, Brazil, diniz@smt.ufrj.

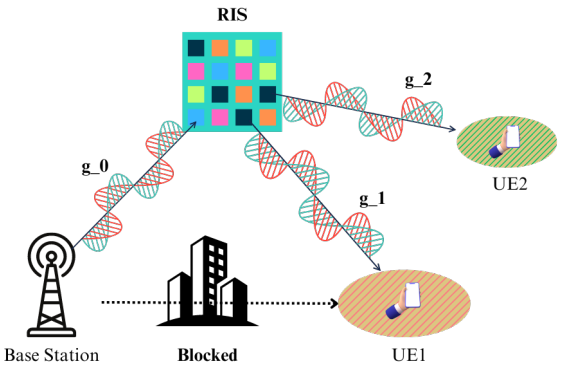

Fig. 1: RIS-assisted NOMA downlink transmission with M = 2 users.

is the power allocation coefficient, for the mth UE. Moreover, we consider $\mathbb{E}[|x_m(n)|^2] = 1$ and

$$\sum_{m=1}^{M} p_m = 1. \tag{2}$$

As depicted in Fig. 1, the line-of-sight (LoS) channel path between BS and the mth UE is blocked. Moreover, we consider fixed both BS and RIS, and moving UEs, albeit their speed is low to avoid Doppler effects. The $x(n)$ is transmitted through the cascaded channel $h_m(n)$, written as

$$h_m(n) = \sqrt{\beta_m(n)}\mathbf{g}_m^{\mathrm{H}}(n)\mathbf{\Theta}\mathbf{g}_0, \tag{3}$$

where $\mathbf{g}_0 \sim \mathcal{CN}(\bar{\mathbf{g}}_0, \mathbf{I}_L)$ is the channel vector between the BS and RIS, $\mathbf{g}_m(n) \sim \mathcal{CN}(\bar{\mathbf{g}}_m, \mathbf{I}_L)$ is the channel vector between the RIS and the mth UE, and $\mathbf{\Theta}$ is the phase shift matrix denoted by

$$\mathbf{\Theta} = \mathrm{Diag}\left(\mathrm{e}^{\mathrm{j}\theta_1}, \mathrm{e}^{\mathrm{j}\theta_2}, \cdots, \mathrm{e}^{\mathrm{j}\theta_L}\right), \tag{4}$$

with $\theta_l \in (-\pi, \pi)$ is the phase shift of the lth element. Additionally, $\beta_m(n)$ is the path loss expressed as

$$\beta_m(n) = \left(\frac{d_{\mathrm{sr}}}{d_0}\right)^{-\alpha_{\mathrm{sr}}} \left(\frac{d_{\mathrm{rm}}(n)}{d_0}\right)^{-\alpha_{\mathrm{rm}}}, \tag{5}$$

where $d_0 \in \mathbb{R}_+$ is the reference distance, $\alpha_{\mathrm{sr}} \in \mathbb{R}_+$ and $d_{\mathrm{sr}} \in \mathbb{R}_+$ are the environment's path loss exponent (PLE) and distance from BS to RIS. α_{rm} and $d_{\mathrm{rm}}(n)$ are the environment's PLE and distance from RIS to the mth UE [19]. In this system, the channel between the BS and RIS varies with each time sample n, while the channel between the RIS and each UE is slowly time-variant due to the movement of the UEs. As both UEs are moving further away from the BS at a constant speed we can infer that the time-space function of $d_{\mathrm{rm}}(n)$ is described by

$$d_{\mathrm{rm}}(n) = d_{\mathrm{rm}}(0) + v_m n, \tag{6}$$

where $d_{\mathrm{rm}}(0) \in \mathbb{R}_+$ is the initial position for the mth UE and $v_m \in \mathbb{R}_+$ is the velocity in m/samples for the mth UE.

The received signal at the mth UE is given by

$$y_m(n) = \sqrt{\rho}h_m(n)x(n) + w_m(n), \tag{7}$$

where $\rho \in \mathbb{R}_+$ is the SNR and $w_m(n) \sim \mathcal{CN}(0, 1)$ is the additive white Gaussian noise (AWGN).

At the weaker UE's single-antenna receiver, the UEs are ordered by signal power strength, enabling the receiver to prioritize and remove stronger signals using SIC. This process decodes and subtracts stronger user signals from the received superposed signal, making it easier to decode the weaker UE's signal by progressively eliminating interference. The weaker UE always decodes the stronger signal first, cancels it from the received signal, and then decodes its transmission, while the stronger UE directly decodes its signal without requiring SIC. Therefore, examining (7), the equation for $y_m(n)$ when performing SIC at UE_m is

$$y_{m,x_m}(n) = y_m(n) - \sum_{i=m+1}^{M} \sqrt{\rho}\hat{h}_m(n)\sqrt{p_i}\hat{x}_i(n), \tag{8}$$

where $\hat{h}_m(n) \in \mathbb{C}$ is the estimated channel for the UE_m.

The joint use of RIS and NOMA systems improves signal quality and coverage. Yet, the substantial number of elements in RIS introduces complexity in channel estimation, thereby limiting the efficacy of traditional methods. This creates an opportunity for the application of DL-based approaches to efficiently estimate channel pilotless [15], [20].

III. Channel Predictor

A. Problem Formulation

As presented in (8), channel state information (CSI) is necessary to perform SIC at the mth UE. In this paper, we propose a DL approach to gather the CSI by predicting the channel in future time steps. The estimated channel in this work is denoted by partial CSI and the perfect channel is called full CSI. Specifically, the estimated channel is given by

$$\hat{h}_m(n) = f(y_m), \tag{9}$$

where $f(\cdot)$ is a nonlinear function modeled by the proposed DL model. Advanced DL approaches, such as CNN and LSTM, address the estimation of nonlinear functions by offering robust feature extraction and sequential data processing, respectively [18], [21]–[23], enabling more accurate and adaptive channel prediction to optimize RIS-NOMA system's performance.

B. Dataset and Feature Extraction

The dataset used to train the proposed architecture comprises two main quantities, the matrices $\mathbf{Y}$ and $\mathbf{H}$, containing the received signals and cascaded channels for the UEs, respectively. The proposed model aims to predict the CSI for adaptability in dynamic conditions by incorporating magnitude and phase as the output of the DL model, unlike in [24], which only uses magnitude as output. This time-series prediction uses previous data points of $\mathbf{Y}$ as inputs in a sliding window manner to forecast future values of $\mathbf{H}$.

The received signal at each UE can be written as

$$\mathbf{y}_m(n) = [y_m(n + t_{\mathrm{i}} - 1)\ y_m(n + t_{\mathrm{i}} - 2)\ \cdots\ y_m(n)]^{\mathrm{T}}, \tag{10}$$

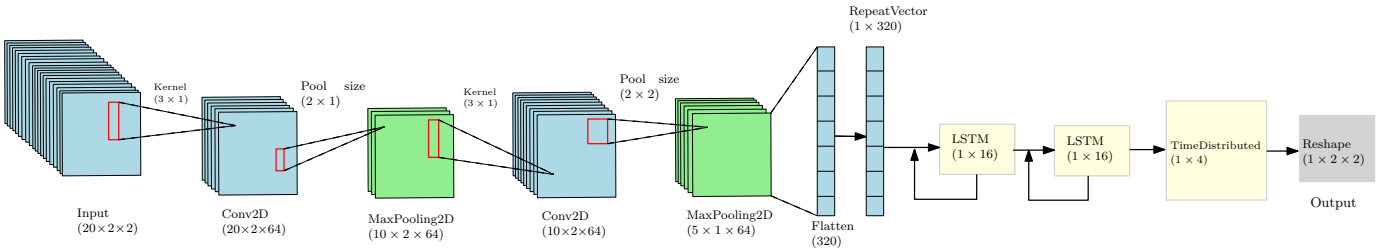

Fig. 2: The CNN-LSTM model architecture visualization.

where $t_{\mathrm{i}} \in \mathbb{N}$ is the input time steps. The vector $\mathbf{y}_m(n)$ predicts the CSI $h_m(n+t_{\mathrm{o}})$ with $t_{\mathrm{o}} \in \mathbb{N}$ being the output time steps. Considering both users, we create the coordinate point $(\mathbf{Y}^{\mathrm{c}}(n), \mathbf{h}^{\mathrm{c}}(n))$, where $\mathbf{Y}^{\mathrm{c}}(n) = [\mathbf{y}_1(n) \ \cdots \ \mathbf{y}_m(n)]$ is the input data and $\mathbf{h}^{\mathrm{c}}(n) = [h_1(n+t_{\mathrm{o}}) \ \cdots \ h_m(n+t_{\mathrm{o}})]$ is the target. In this formulation, the N time steps cannot be used because the first $t_{\mathrm{i}}-1$ samples lack enough prior data, and the last few samples lack future output data. Thus, we used the variable $N' = N - t_i - t_o + 1$ to represent the total number of samples in the dataset.

Since $\mathbf{y}_m(n)$ and $h_m(n+t_{\mathrm{o}})$ are complex numbers, we separate the phase and magnitude into different dimensions for compatibility with conventional DL models. Thus, $\mathbf{Y}^{\mathrm{c}}(n)$ and $\mathbf{h}^{\mathrm{c}}(n)$ are transformed into tensors $\mathbf{Y}(n)$ and $\mathbf{H}(n)$, where the first slabs are $\mathbf{Y}_1(n) = |\mathbf{Y}^{\mathrm{c}}(n)|$ and $\mathbf{H}_1(n) = |\mathbf{h}^{\mathrm{c}}(n)|$, and the second slabs are $\mathbf{Y}_2(n) = \angle\mathbf{Y}^{\mathrm{c}}(n)$ and $\mathbf{H}_2(n) = \angle\mathbf{h}^{\mathrm{c}}(n)$. The dataset is given by

$$\mathcal{D} = \{(\mathbf{Y}(1), \mathbf{H}(1)), \ \cdots, \ (\mathbf{Y}(N'), \mathbf{H}(N'))\}, \tag{11}$$

where $\mathbf{Y}(n) \in \mathbb{R}^{t_{\mathrm{i}} \times M \times 2}$ and $\mathbf{H}(n) \in \mathbb{R}^{1 \times M \times 2}$, account for the time samples used for prediction, number of users, and magnitude–phase, respectively. In this paper, the proposed model uses $t_i = 20$ time steps to predict $t_o = 1$.

C. Proposed Architecture

The DL architecture in [24] uses two Conv2D layers for feature mapping, followed by a max-pooling layer to reduce complexity and noise sensitivity. On the other hand, the proposed model introduces a max-pooling layer after the first Conv2D operation, using different pool sizes to improve feature extraction and reduce the computational burden. This dual-pooling approach improves feature recognition and reduces the model's computational burden. The CNN, with 64 filters, a $(3,1)$ kernel, and rectified linear unit activation, outputs to the LSTM module, which captures temporal dependencies for accurate channel estimation. A RepeatVector layer adjusts the output for LSTM input, and two LSTM layers with 16 memory cells process the data. The Time Distributed Dense layer refines the sequence, and the model is trained using the Adam optimizer with mean squared error (MSE) as the loss function. The convolutional layers in particular were achieved by a grid search combination for $F_{\mathrm{filter}} \in \{4, 8, 16, 64\}$ considering both the training loss and accuracy results. Figure 2 depicts the proposed model operational layers for $M = 2$.

D. Computational Complexity

The proposed model input does not scale with the number of RIS elements, since the CNN-LSTM architecture input does not depend on the number of RIS elements L. The architecture complexity would not be affected by an infinite number of RIS elements. The number of RIS elements only affects the cascade channel distribution due to (3), demanding retraining for RIS with different element numbers. On the other hand, the complexity would increase with the number of time steps t_i and the number of users M. Increasing t_i would increase the size of the input layer, and increasing M would potentially increase the size of all convolutional layers and the number of layers in the model. However, an increased t_i potentially leads to better prediction since the model would have more data available to provide an output. Furthermore, it is worth mentioning that with different parameters, it would be possible to design a completely different architecture with a better trade-off in terms of performance and complexity.

IV. Simulation Results

To evaluate the DL model, we used key performance metrics as in [24], including normalized root mean squared error (NRMSE), mean absolute scaled error (MASE), mean absolute percentage error (MAPE), root mean squared error (RMSE), mean absolute error (MAE), and R-squared score (R^2 score). All the codes used in this paper are available on GitHub.[1] We considered a BS aided by a RIS with $L = 20$ elements transmitting 4-quadrature amplitude modulation (QAM) symbols to $M = 2$ UEs during $N = 20000$ samples. The RIS is $d_{\mathrm{sr}} = 150$ m apart from the BS, the UEs are initially $d_{\mathrm{r1}}(0) = 30$ m, and $d_{\mathrm{r2}}(0) = 40$ m from the RIS, moving away from it at a speed of $v = 0.01$ m/sample, and the reference distance is $d_0 = 20$ m. Channels are modeled as $\mathbf{g}_0(n) \sim \mathcal{CN}(1,1)$, $\mathbf{g}_1(n) \sim \mathcal{CN}(4,1)$, and $\mathbf{g}_2(n) \sim \mathcal{CN}(3,1)$. The system has an amplitude reflection coefficient $\alpha_m = 1$, the phase shift $\theta_l = 0.01\pi + (l-1)0.01\pi/L$ as employed in [24], and PLE coefficients of 2.2 for all links. The SNR is $\rho \in \{-10, -5, 0, \cdots, 35\}$ dB and power allocation factors are $p_1 = 0.3$ and $p_2 = 0.7$. Additionally, we split the data sequentially, using a ratio of 0.8:0.2 for training and testing. Table I summarizes the parameters used in the simulation.

Fig. 3 shows the magnitude and phase of the cascaded channel for UE_1 over time in samples, highlighting the DL model's

[1] https://github.com/eduardo-henriques/Deep-Learning-based-Channel-Predictor-for-RIS-assisted-NOMA-Communication-Systems

TABLE I: Two-user scenario dataset parameters.

Parameter	Description
$N = 20000$	Number of time steps
$M = 2$	Number of users
$L = 20$	Number of RIS elements
$v = 0.01$ m/time step	Speed of users
$\rho \in \{-10, -5, \cdots, 35\}$ dB	SNR
$\mathbf{g}_0 \sim \mathcal{CN}(1, 1)$	Channel between BS and RIS
$\mathbf{g}_1 \sim \mathcal{CN}(4, 1)$	Channel between BS and UE_1
$\mathbf{g}_2 \sim \mathcal{CN}(3, 1)$	Channel between BS and UE_2
$d_0 = 20$ m	Reference distance
$d_{sr} = 150$ m	Distance from BS to RIS
$d_{s1}(0) = 30$ m	Distance from RIS to UE_1
$d_{s2}(0) = 40$ m	Distance from RIS to UE_2
$\alpha_m = 1$	Amplitude reflection coefficient
$\theta_l = 0.01\pi + (l-1)0.01\pi/L$	RIS phase shift
$\alpha_{r1} = 2.2$	PLE from RIS to UE_1
$\alpha_{r2} = 2.2$	PLE from RIS to UE_2
$\alpha_{sr} = 2.2$	PLE from BS to RIS
$p_1 = 0.3$	Power allocation for UE_1
$p_2 = 0.7$	Power allocation for UE_2
$t_i = 20$	Number of input time steps
$t_o = 1$	Number of output time steps

predictive performance for $\rho = 30$ dB. In Fig. 3a, the true cascaded channel magnitude and the model's prediction are compared, with a zoomed section that showcases the model's performance on unseen data and its ability to capture the channel's magnitude. Fig. 3b illustrates the phase prediction, where initial discrepancies in prediction decrease as learning progresses. These results highlight the challenges and potential of using deep learning for accurate channel modeling in RIS-aided NOMA systems. Similar results were observed for UE_2 under the same conditions, indicating the model's consistent performance in predicting both magnitude and phase in RIS-NOMA systems.

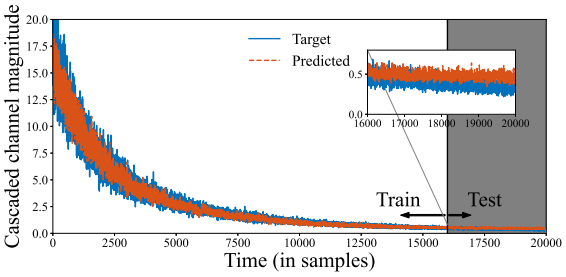

(a) Magnitude.

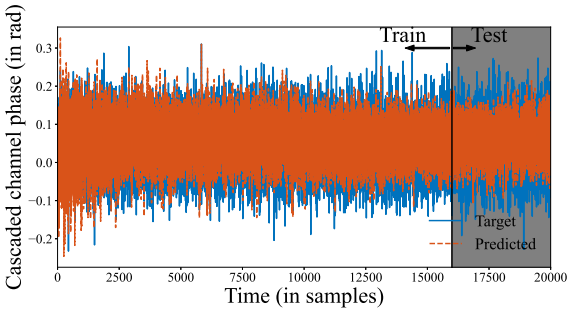

(b) Phase.

Fig. 3: UE_1's cascaded channel prediction for SNR = 30 dB.

TABLE II: Performance metrics of different DL models for $\rho = 30$ dB.

Metrics	Model proposed in [24]	Proposed model
NRMSE	0.098	0.096
MASE	0.063	0.057
MAPE	468.485	163.640
R^2 score	0.910	0.925
RMSE	0.089	0.077
MAE	0.073	0.063
Inference time	0.409 ms	0.338 ms
Trainable parameters	57028 (222.77 KB)	36548 (142.77 KB)

Fig. 4 compares the BER performance for two UEs under partial and full CSI knowledge across SNR values, where full CSI knowledge is knowledge of the perfect channel and partial CSI knowledge is knowledge of the predicted channel. The BER was calculated for each time step and averaged over the test dataset for each SNR. While full CSI knowledge provides lower BER, the performance with partial CSI obtained from the proposed architecture remains close, especially at low-SNR regime. This demonstrates the model's effectiveness in predicting critical channel characteristics, maintaining a competitive BER even with limited channel information.

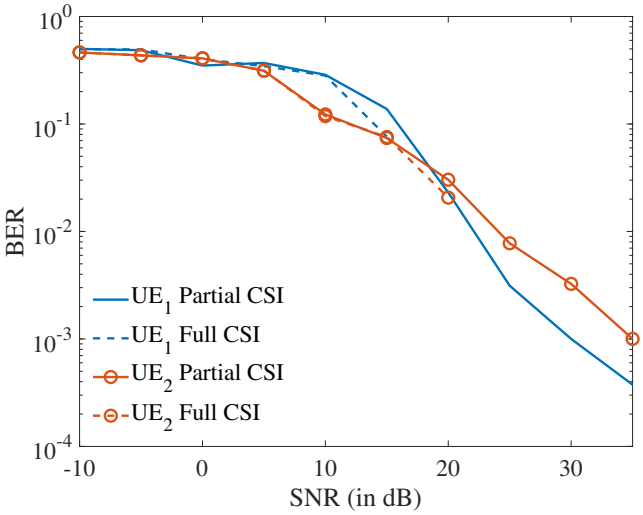

Fig. 4: BER *versus* SNR for 100 epochs.

We compared the proposed DL-based channel predictor to the state-of-the-art model from [24], referred to as the "baseline model". As shown in Table II, the proposed model outperforms the baseline across all the evaluated metrics, demonstrating better accuracy and fewer errors. Moreover, it is worth noting that the proposed model reduces the average inference time and trainable parameters by 17% and 35.9%, respectively. This result confirms that the proposed model is more efficient in computation and memory, which is critical for real-time processing. Furthermore, in Fig. 5, the proposed model achieved at least the same BER compared to the baseline at low-SNR regime for both UEs. On the other hand, at high-SNR regime, UE_1 achieved a BER of 10^{-3} at $\rho \sim 30$ dB by using the proposed model, yielding a SNR gain of ~ 5 dB over the baseline for the same BER.

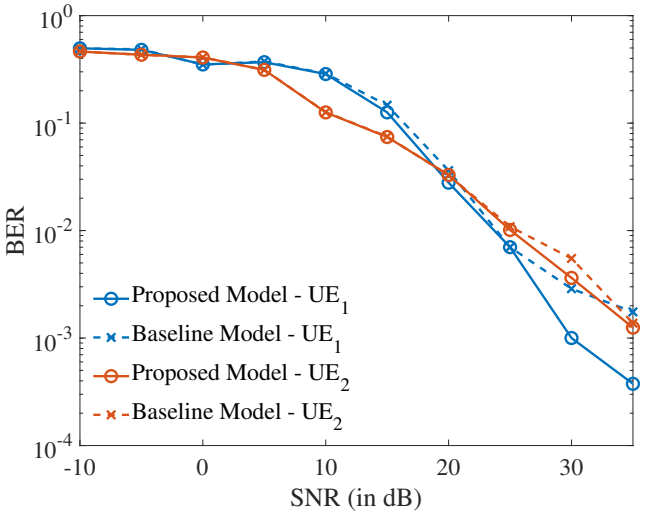

Fig. 5: BER *versus* SNR for different models.

V. Conclusion

This paper provided a comprehensive analysis on the integration of NOMA and RIS, highlighting the transformative potential of DL solutions to estimate the channel of a wireless system. The proposed DL-based channel predictor outperformed the baseline model, our main goal, and successfully replicated the time-series patterns of channel magnitude and phase for both UEs. These results, along with the promising BER performance over SNR, demonstrate the robustness and reliability of the predictor for a single antenna RIS-NOMA downlink system.

Future work shall focus on further optimizing the DL model by reducing its complexity, possibly through fewer LSTM layers or improved hyperparameter tuning, and refining the dataset generation process. Furthermore, it shall explore more advanced modulation schemes, incorporating realistic scenarios such as higher UEs speeds with Doppler effects, including direct BS-to-UE paths, and adapting the architecture to multiple-input multiple-output (MIMO) environments with multiple UEs and antennas. Additionally, developing decentralized predictors for individual UEs and extending the channel prediction framework to RIS-NOMA systems in uplink transmission would provide valuable insights and broaden the applicability to emerging internet of things (IoT) and sensing applications.

Acknowledgment

This study was financed by FAPERJ - Fundação de Amparo à Pesquisa do Estado do Rio de Janeiro, Projeto FAPERJ E-26/210.157/2023. The Brazilian Research Councils CAPES and CNPq have also supported this work.

References

[1] W. Jiang, B. Han, M. A. Habibi, and H. D. Schotten, "The Road Towards 6G: A Comprehensive Survey," *IEEE Open J. Commun. Soc.*, vol. 2, pp. 334–366, Dec. 2021.

[2] P. Popovski, K. F. Trillingsgaard, O. Simeone, and G. Durisi, "5G Wireless Network Slicing for eMBB, URLLC, and mMTC: A Communication-Theoretic View," *IEEE Access*, vol. 6, pp. 55 765–55 779, Sep. 2018.

[3] R. Chataut, M. Nankya, and R. Akl, "6G Networks and the AI Revolution—Exploring Technologies, Applications, and Emerging Challenges," *Sensors*, vol. 24, no. 6, p. 1888, Mar. 2024.

[4] M. Mahbub and R. M. Shubair, "Investigation of the Intelligent Reflecting Surfaces-Assisted Non-Orthogonal Multiple Access in 6G Networks," in *IEEE 13th Annual Information Technology, Electronics and Mobile Communication Conference*, on-line event, Oct. 2022, pp. 0492–0496.

[5] M. Vaezi, A. Azari, S. R. Khosravirad, M. Shirvanimoghaddam, M. M. Azari, D. Chasaki, and P. Popovski, "Cellular, Wide-Area, and Non-Terrestrial IoT: A Survey on 5G Advances and the Road Toward 6G," *IEEE Commun. Surv. Tutorials*, vol. 24, no. 2, pp. 1117–1174, Sep. 2022.

[6] B. Patnaik, A. Agarwal, S. Mali, G. Misra, and K. Agarwal, "A Review on Non-Orthogonal Multiple Access Technique for Emerging 5G Networks and Beyond," in *International Conference on Smart Electronics and Communication*, Trichy, India, Sep. 2020, pp. 698–703.

[7] A. Jamalipour, T. Wada, and T. Yamazato, "A Tutorial on Multiple Access Technologies for Beyond 3G Mobile Networks," *IEEE Commun. Mag.*, vol. 43, no. 2, pp. 110–117, Feb. 2005.

[8] J. Li, X. Wu, and R. Laroia, *OFDMA Mobile Broadband Communications: A Systems Approach*. Cambridge University Press, Jul. 2013.

[9] C. Pan, H. Ren, K. Wang, J. F. Kolb, M. Elkashlan, M. Chen, M. Di Renzo, Y. Hao, J. Wang, A. L. Swindlehurst, X. You, and L. Hanzo, "Reconfigurable Intelligent Surfaces for 6G Systems: Principles, Applications, and Research Directions," *IEEE Commun. Mag.*, vol. 59, no. 6, pp. 14–20, Jul. 2021.

[10] C. Huang, A. Zappone, G. C. Alexandropoulos, M. Debbah, and C. Yuen, "Reconfigurable Intelligent Surfaces for Energy Efficiency in Wireless Communication," *IEEE Trans. Wireless Commun.*, vol. 18, no. 8, pp. 4157–4170, Aug. 2019.

[11] E. Björnson and Ö. Demir, *Introduction to Multiple Antenna Communications and Reconfigurable Surfaces*. Now Publishers Inc., Jan. 2024.

[12] L. Li, L. He, Y. Li, and P. S. R. Diniz, "Robust RIS-based DOA Estimation with Mixed Constraints," *IEEE Signal Process. Lett.*, vol. 31, pp. 2260 – 2264, Aug. 2024.

[13] T. Hou, Y. Liu, Z. Song, X. Sun, Y. Chen, and L. Hanzo, "Reconfigurable Intelligent Surface Aided NOMA Networks," *IEEE J. Sel. Areas Commun.*, vol. 38, no. 11, pp. 2575–2588, Nov. 2020.

[14] A. Salh, L. Audah, N. S. M. Shah, A. Alhammadi, Q. Abdullah, Y. H. Kim, S. A. Al-Gailani, S. A. Hamzah, B. A. F. Esmail, and A. A. Almohammedi, "A Survey on Deep Learning for Ultra-Reliable and Low-Latency Communications Challenges on 6G Wireless Systems," *IEEE Access*, vol. 9, pp. 55 098–55 131, Mar. 2021.

[15] M. Haghshenas, "Passive Reconfigurable Intelligent Surfaces: Efficient Channel Estimation and Codebook Design," Ph.D. dissertation, Politecnico di Milano, Mar. 2024.

[16] H. Ye, G. Y. Li, and B.-H. Juang, "Power of Deep Learning for Channel Estimation and Signal Detection in OFDM Systems," *IEEE Wireless Commun. Lett.*, vol. 7, no. 1, pp. 114–117, Sep. 2018.

[17] H. A. Alzubaidi L., Zhang J., "Review of Deep Learning: Concepts, CNN Architectures, Challenges, Applications, Future Directions." *Journal of Big Data*, vol. 8, no. 1, p. 53, Mar. 2021.

[18] S. Hochreiter and J. Schmidhuber, "Long Short-Term Memory," *Neural Computation*, vol. 9, no. 8, pp. 1735–1780, Dec. 1997.

[19] J. Miranda, R. Abrishambaf, T. Gomes, P. Gonçalves, J. Cabral, A. Tavares, and J. Monteiro, "Path loss exponent analysis in Wireless Sensor Networks: Experimental evaluation," in *11th IEEE International Conference on Industrial Informatics*, Bochum, Germany, Jul. 2013, pp. 54–58.

[20] F. Ait Aoudia and J. Hoydis, "End-to-End Learning for OFDM: From Neural Receivers to Pilotless Communication," *IEEE Trans. Wireless Commun.*, vol. 21, no. 2, pp. 1049–1063, Feb. 2022.

[21] J. Gu, Z. Wang, J. Kuen, L. Ma, A. Shahroudy, B. Shuai, T. Liu, X. Wang, and G. Wang, "Recent Advances in Convolutional Neural Networks," *arXiv preprint arXiv: 1512.07108*, vol. abs/1512.07108, Dec. 2015.

[22] A. Khan, A. Sohail, U. Zahoora, and A. S. Qureshi, "A Survey of the Recent Architectures of Deep Convolutional Neural Networks," *arXiv preprint arXiv: 1901.06032*, Jan. 2019.

[23] D. G. Lui, G. Tartaglione, F. Conti, G. De Tommasi, and S. Santini, "Long Short-Term Memory-Based Neural Networks for Missile Maneuvers Trajectories Prediction," *IEEE Access*, vol. 11, pp. 30 819–30 831, Mar. 2023.

[24] C. Nguyen, T. M. Hoang, and A. A. Cheema, "Channel estimation using cnn-lstm in ris-noma assisted 6g network," *IEEE Trans. Mach. Learn. Commun. and Netw.*, vol. 1, pp. 43–60, May 2023.